

# Effect of Inorganic Nanomaterials Types Functionalized with Smart Nanogel on Anti-corrosion and Mechanical Performances of Epoxy Coatings

Ayman M. Atta<sup>1,2,\*</sup>, Ashraf M. El-Saeed<sup>2</sup>, Hussin I. Al-Shafey<sup>2</sup>, Hamad A. Al-Lohedan<sup>1</sup>, Ahmed M. Tawfeek<sup>3</sup> and Mohamed Wahbey<sup>1</sup>

<sup>1</sup> Surfactants research chair, Chemistry department, college of science, King Saud University, Riyadh 11451, Saudi Arabia.

<sup>2</sup> Petroleum Application Department, Egyptian Petroleum Research Institute, Nasr City 11727, Cairo, Egypt.

<sup>3</sup> college of science, King Saud University, Riyadh 11451, Saudi Arabia.

\*E-mail: [aatta@ksu.edu.sa](mailto:aatta@ksu.edu.sa)

Received: 17 October 2016 / Accepted: 7 December 2016 / Published: 30 December 2016

---

Nanomaterials based on metal oxides play an important role to fill the micro-cracks and porosity of epoxy coats but fail to act as self-healing for damage coats. In the present work, the surfaces of metal oxides such as titania, silica and montmorillonite nanomaterials were modified with smart crosslinked copolymers based on N-isopropylacrylamide monomer (NIPAm) by surfactant free dispersion polymerization technique. The surface morphology, particle size distributions, surface charges and nanogel contents of the prepared composites were investigated to study the effect of modification on the dispersion stability of metal oxide nanoparticles. The modified nanogel composites were blended with epoxy matrix in curing process with polyamide hardener at different concentrations to study the surface properties of modified epoxy coats. The incorporation of nanogel composites with epoxy enhances the mechanical properties and anticorrosion behavior of epoxy resins as coat for steel substrate.

---

**Keywords:** Epoxy coats; Salt spray; Mechanical properties; Corrosion; Nanogel composites.

## 1. INTRODUCTION

Nanomaterials became the most important materials used to modify the surfaces of different metal substrates such as pigments, coat, organic coating modifiers and filler to protect them from aggressive corrosion environments [1-5]. These materials can protect the metal corrosion through different mechanisms such as barrier, sacrificial, inhibitive, self-healing materials for damaged organic

coatings and behave as nanocontainer for corrosion inhibitors or as smart materials to form new bonds at damaged area to protect the metal from corrosive media [6-9]. There are different types of nanomaterials have been widely used to modify the surface properties of organic coats such as zirconia, titania, silica, alumina, cerium, clay minerals, iron oxide etc. [10-14]. The limitations of these nanomaterials to apply as anti-corrosive materials depend on their shapes, sizes, stability to pH variations, dispersability in coats without formation cluster of aggregates and chemical structure of nanomaterials. The chemical modification routes attracted great attention to control the shape, sizes and dispersability of different types of nanoparticles. Among different routes of chemical modifications, the conversion of metal or metal oxides nanoparticles to amphiphilic nanogel composites attracted great attention to modify the dispersability, shapes and sizes of nanoparticles [15-18]. It is preferred over other surface modifications pathways because it can modify both the anticorrosion and mechanical performances of nanomaterials due to formation of flexible, intelligent and highly dispersed nanocomposites when blended with organic coats.

Intelligent nanomaterials have a properly engineered combination of changes of their properties with their response to external stimuli variation are very useful for applications as coats [19-23]. The surface modification of inorganic nanoparticles with intelligent materials to form intelligent core/shell morphology is useful technique to control their surface properties. These hybrid core/shell nanomaterials possess unique combination between smart characteristic of nanogel and nano activity of inorganic materials. These surfaces can reversibly change their performance between, for example, adhesive and non-adhesive, conductive and nono-conductive, and super-hydrophobic and super-hydrophilic, and conductive and insulator states [24-26]. The smart core/shell nanogel inorganic nanoparticles can form self-assembled thin films when deposited on the substrate surfaces to form monolayer film has superior anti-corrosion performances when it exposed to corrosive environments [27-30]. Moreover, the smart core/ shell inorganic nanogel materials can act as “intelligent” self-healing and anticorrosion coatings to release the inhibitors when the coat damaged and return to the sealed state after elimination of corrosive environments [31]. In our previous works [32-36], N-isopropyl acrylamide (NIPAm) attracted considerable interest to modify the surface of inorganic nanomaterials and to prepare amphiphilic nanogel particle having superior surface activity to form self-assembled monolayers. In the present work, NIPAm nanogel polymer is used to modify the surface of commercially available inorganic nanomaterials based on clay mineral, silica and titanium dioxide to investigate the effect of inorganic nanomaterial types on their performances as anticorrosion and mechanical properties for epoxy coating modifiers. The corrosion resistance of modified epoxy coats with different types of nanogel inorganic composites was studied by salt spray test beside adhesion and mechanical measurements.

## 2. EXPERIMENTAL

### 2.1. Materials

A hydrophilic silica nanoparticle have particle sizes ranged from 15-25 nm and degree of hydrolysis 100 % was a gift from Eka Chemicals., Titanium dioxide ( $\text{TiO}_2$ ; nano-powder has average

particle size 21 nm), hydrophilic sodium montmorillonite (commercial name `Nanomer ® PGV; Na-MMT) N-isopropyl acrylamide (NIPAm), acrylic acid (AA), *N,N*-methylenebisacrylamide (MBA) crosslinker, ammonium persulfate radical polymerization initiator (APS), *N,N,N',N'*-tetramethylethylenediamine radical polymerization activator (TEMED) and poly(vinyl pyrrolidone) stabilizer (PVP with molecular weight 40,000 g/mol) were obtained from Sigma-Aldrich Co. *The commercial epoxy resin SigmaGuard™ CSF 650 produced by Sigma Coatings, SigmaKalon Group were applied as epoxy coats for steel.*

## 2.2. Preparation of NIPAm/AA nanogel composites:

Silica, TiO<sub>2</sub> or Na-MMT nanoparticles (3.5 g) were dispersed in (150 mL) of ethanol/ water mixture (60/40 vol %) and (1 g) PVP as stabilizing agent with stirring for 24 h at room temperature. NIPAm and AA were copolymerized with mol ratio 1. NIPAm (0.3 g) was added to the reaction mixture with 0.0125 g KPS initiator, and 20 µl TEMED at temperature of 40 °C after bubbling with nitrogen atmosphere under stirring. The reaction temperature keep constant for 1h until the solution turned to be turbid or cloudy. The remained NIPAm (0.5 g), AA (0.7 g) and MBA ( 0.144 g) were dissolved into 20 mL of water were introduced into the reaction mixture for 30 minutes. The reaction temperature increased to 55 °C and keeps constant for 24 h. The nanogel composites were separated from the solutions after ultracentrifuge at 21000 rpm for 30 minute and purified using dialysis membrane for 1 week.

## 2.3. Preparation of epoxy nanocomposite coats

Na-MMT-NIPAm/AA, TiO<sub>2</sub>-NIPAm/AA and silica-NIPAm/AA nanogel composites were mixed with different weight percentages ranged from 0.1 to 3 wt.% based on total weight of epoxy and hardener. The epoxy nanogel blends were mixed with 8 mL of epoxy resins and sonicated for 30 min. The dispersed epoxy nanogel composites were added to polyamine hardener (2 mL) under vigorous stirring. The epoxy polyamide hardener mixtures were sprayed on blasted and cleaned steel panels to obtain dry film thickness (DFT) of 100 µm. The coated panels stored at temperature 40 °C to be sure the all epoxy films were cured to complete tests.

## 2.4. Characterization

The thermal stability and nanogel contents of nanogel composites were evaluated using thermogravimetric analysis (TGA; TGA-50 SHIMADZU at flow rate 50 ml/min and heating rate of 20 °C / min).

The surface morphology of nanogel composite was examined using high resolution transmission electron microscope (HR-TEM using a JEOL JEM-2100 electron microscope at an acceleration voltage of 200 kV).

The dispersion stability, polydispersity index (PDI) and surface charges (zeta potential; mV) of nanogel composites were determined by using dynamic light scattering (DLS; Laser Zeta meter Malvern Instruments; Model Zetasizer 2000).

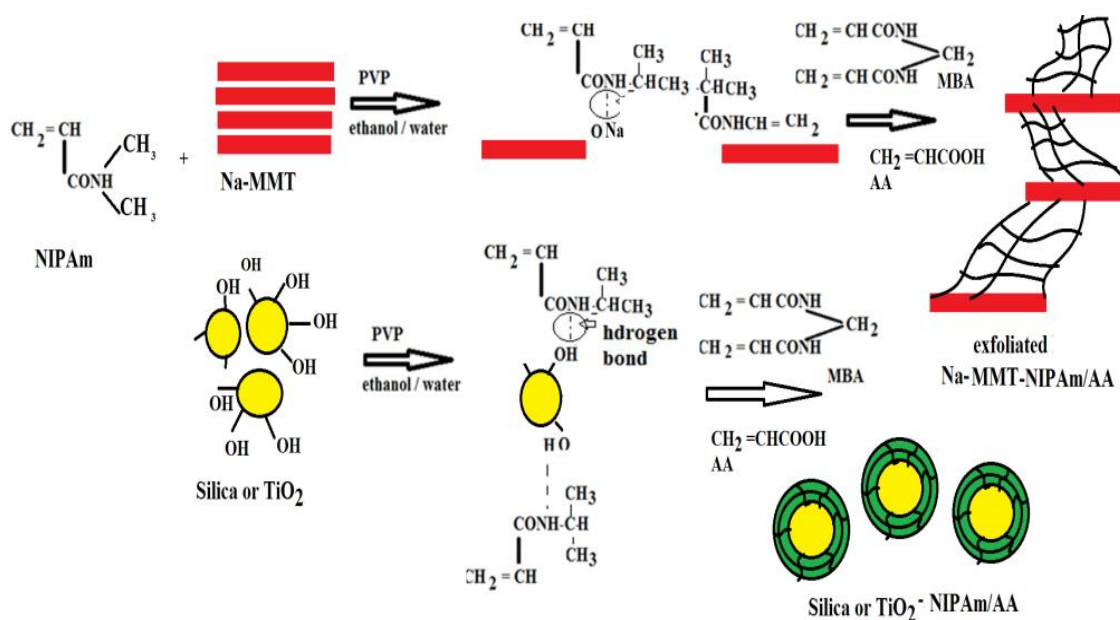
The surface contact angles between cured epoxy panels were determined using drop shape analyzer model DSA-100 (the temperature and moisture were 23°C and 68% respectively).

The distribution of nanogel composites into cured epoxy films was examined using optical microscope ( Olympus DP 72 ) after coating the glass slides with epoxy nanogel composites.

All mechanical tests of coated steel panels such as abrasion resistance, hardness, T-bending, impact resistance, and pull-off adhesion test were evaluated according standard methods ASTM. A salt spray cabinet (manufactured by CW Specialist equipment ltd. model SF/450) was used to determinethe salt spray resistance of coated panels.

### 3. RESULTS AND DISCUSSIONS

The present work aims to modify the surface properties of some inorganic oxide nanoparticles such as silica, TiO<sub>2</sub> and Na-MMT to increase their dispersability into epoxy matrix to improve both mechanical properties and anticorrosion performance against marine environments. In this respect, the mechanism of modification is illustrated in **Scheme 1**.



**Scheme 1.** Synthesis of metal oxide nanogel composites.

The mechanism is based on using two monomers, one is smart monomer based on NIPAm that contains both hydrophobic moiety (isopropyl group) and hydrophilic moiety (amide group) and the second is AA which has carboxylic group that sensitive to pH variation. The polymerization of these monomers in the presence of MBA crosslinker, APS radical initiator and TEMED as activator can

encapsulate inorganic metal oxide nanoparticle into nanogel composites [37-40]. The crosslinking copolymerization is carried out using surfactant free dispersion polymerization technique. Approximately 0.3 mol% of NIPAm monomer introduced to disperse metal oxide nanoparticles in the presence of PVP stabilizer and ethanol/water (60/40 vol %) as dispersion solvent. The NIPAm can diffuse to surround the metal oxide nanoparticles above its lower critical solution transition temperature (LCST > 39 °C). This was referred to the hydrophobic interaction between isopropyl groups above LCST [40]. The intercalation of Na-MMT gallery and dispersion between nanoparticle increase to facilitate the diffusion of MBA, AA and remained NIPAm monomer to form crosslinked nanogel either to surround the nanoparticles or to exfoliate the galleries as represented in Scheme 1.

### 3.1. Characterization of nanogel composites

The surface morphology of the prepared silica, TiO<sub>2</sub> and Na-MMT nanogel composite with NIPAm/AA is determined by TEM and illustrated in micrograph in Figure 1 a- f. The surface morphology of the modified nanogel composites confirmed the formation of core/shell morphology in which the metal oxide particles as core and nanogel layer as shell. It was also observed that the dispersion of TiO<sub>2</sub> nanogel increased with the surface modification with NIPAm/AA (Figure 1a and b). While the modification of silica surfaces tends to form non-connected particles with formation of smaller nanogel composite aggregates (Figure 1 c and d). The formation of exfoliated Na-MMT-NIPAm/AA nanogel is confirmed from Figure 1 e and f. It was also observed that there is no any nanogel or metal oxide nanoparticles formed separately as confirmed from Figure 1 b, d and f. These results confirmed that the surface of nanogel composites are charged with same charges and repelled to form dispersed nanogel composites and the thickness of nanogel composite layers affects the performance of the formed nanogel composites.

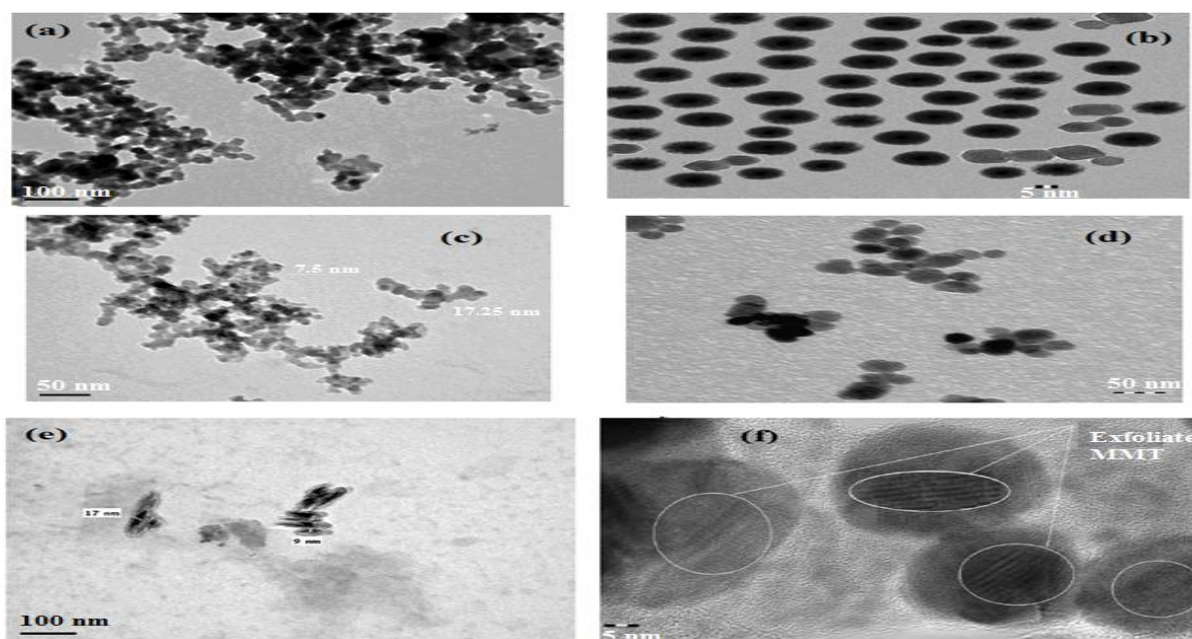


**Figure 1.** TEM micrographs of a) TiO<sub>2</sub>, b) TiO<sub>2</sub>-NIPAm/AA, c)Silica , d) silica-NIPAm/AA, e) Na-

MMT and f) Na-MMT-NIPAm/AA nanomaterials.

The contents of NIPAm/AA nanogel in the prepared silica, TiO<sub>2</sub> and Na-MMT can be determined from TGA thermograms and gathered in Table 1. The weight loss % at temperature ranged from 25 to 250 °C of silica, TiO<sub>2</sub> and Na-MMT nanoparticles are 13, 5 and 8 Wt. %, respectively. It was related to bound water and hydroxyl groups at surface of silica, TiO<sub>2</sub> and Na-MMT nanoparticles which have greater ability to absorb water on their surfaces due to their nano sizes and higher contact area [41]. The another weight loss ranged from 350 to 650 °C can be used to determine the amount of decomposed nanogel composites surrounded to the silica, TiO<sub>2</sub> and Na-MMT nanoparticles as listed in Table 1. The data confirmed that the content of nanogel for silica, TiO<sub>2</sub> and Na-MMT nanoparticles are 31, 47 and 52 %. These data confirm that the silica surrounded with lower amount of NIPAm/AA nanogel than TiO<sub>2</sub> and Na-MMT nanoparticles. These results confirm the shell thickness surrounded to TiO<sub>2</sub> and Na-MMT nanoparticles as represented in Figure 1b, d and f. It can also calculate the crosslinking copolymerization % from the amount of monomers used with monomers feed ratios and that determined from TGA analysis. The crosslinking degree % are increased in NIPAm/AA nanogel in order Na-MMT > TiO<sub>2</sub> > silica nanoparticles.

**Table 1.** TGA data of NIPAm/AA nanogels with TiO<sub>2</sub> and Na-MMT nanoparticles.

Nanogels	Remaining		amounts of nanogel relate metal oxide nanoparticles (Wt%)		Crosslinking copolymerization %
	Temperature range (°C)	Weight loss (%)	Actual	determined	
Na-MMT	25-350	8	-		-
	350-650	-			
Na-MMT-NIPAm/AA	25-275	8	54	52	96.3
	350-650	52			
silica	25-300	7			
	300-650	6			
Silica-NIPAm/AA	25-300	9	52	31	87.2
	300-650	35			
TiO <sub>2</sub>	25-250	4			
	250-650	1			
TiO <sub>2</sub> -NIPAm/AA	25-250	6	52	47	90.4
	250-650 °C	46			

The effect of salt on the dispersion and aggregation of nanoparticles can be determined from DLS measurements in distilled and filtered sea water as represented in Figure 2 a-d and gathered in

Table 2. The polydispersity index (PDI) can be used to confirm that the formation of polydisperse nanoparticles or monodisperse uniform nanoparticles if PDI values are above or below or as small as possible 0.7 [42]. Careful inspection of data confirmed that the PDI and particle size values (Table 2 and Figure 2 a-d) decrease in sea water more than distilled water. These mean that the NIPAm/AA shell has greater tendency to absorb water due to inadequate crosslinking degree of shell that increases the particle diameter and PDI values [43, 44]. It is also reported that, increment of PDI values of nanoparticles may have been caused by inter-particle crosslinking reaction between some adjacent nanoparticles that reflect on wide increment of particle size distribution of nanomaterials [44]. The data also proved that, the high crosslinking density of NIPAm/AA shell reduces the particle sizes and PDI values as confirmed from lower particle sizes of silica and titania NIPAm/AA nanogel composites (Table 2). The sensitivity of NIPAm/AA shell to salt can be referred to hydrophobic interaction of isopropyl group when the salt concentration increased and also attributed to salt screening effect on COOH ionization of AA [45]. The low absorption of NIPAm/AA nanogel in the prepared silica, TiO<sub>2</sub> and Na-MMT to sea water and their high particles dispersion enhance the application of these composite as anticorrosive nanomaterials in marine environments.

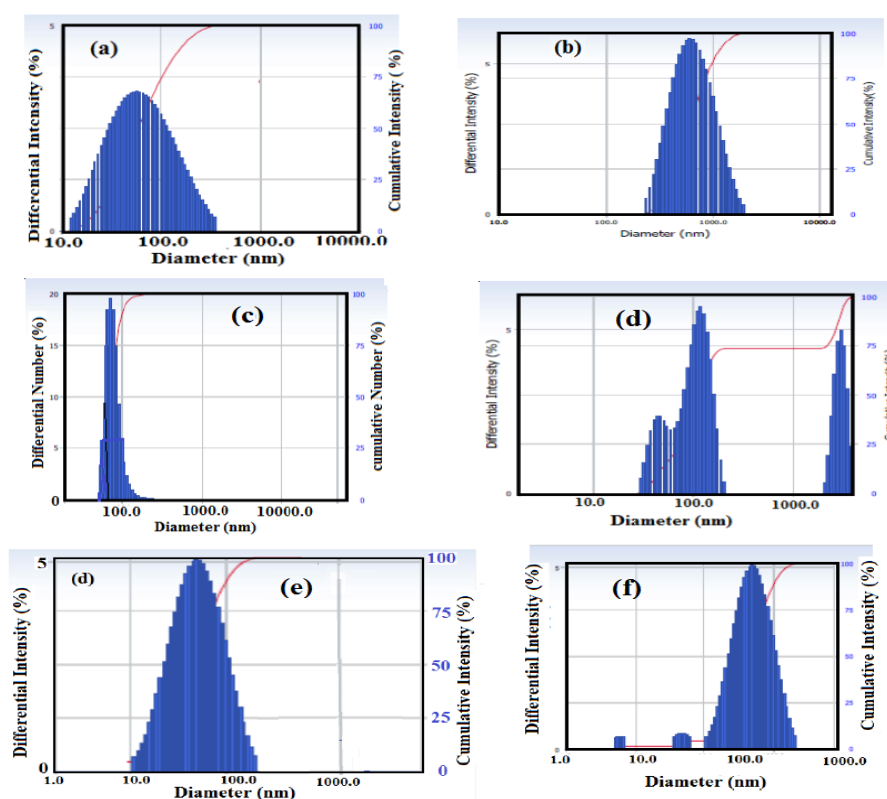


**Figure 2.** DLS measurements of a), b) Na-MMT-NIPAm/AA, c), d) silica-NIPAm/AA, e) and f) TiO<sub>2</sub>-NIPAm/AA in filtered sea and distilled water, respectively.

It is also important to determine and investigate the effect of pH on surface charges of nanomaterials based on silica, TiO<sub>2</sub> and Na-MMT surface modified with NIPAm/AA nanogels. The surface charges are determined from zeta potential ( $\zeta$ - potential; mV) as determined from the experimental section and listed in Table 2 and Figure 3. The data listed in Table 2 confirmed that silica



nanocomposite showed the highest negative surface charges at different pH values ( low negative value; below -25 mV) which confirms that the crosslinked NIPAm/AA shell has lower thickness than other titania or Na-MMT nanoparticles. The high shells thickness may have contained the nanoparticles most effectively intact and prevented the possible breakdown [46, 47]. The pH dependent  $\zeta$ -potential values (Figure 3) can be used to determine the pH isoelectric point (pI) as listed in Table 2.

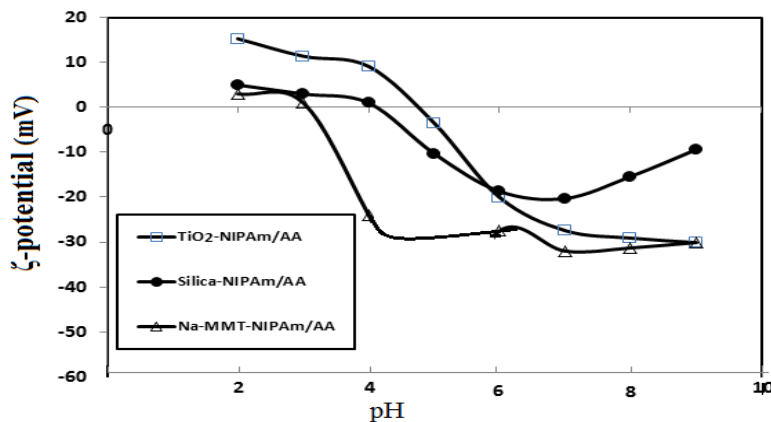


**Figure 3.** Relation between zeta potential of the prepared nanogel composites and pH of aqueous solution at temperature of 25 °C.

**Table 2.** The DLS and Zeta Potential measurements of the nanogel composites.

NIPAm/AAm nanogels	solvent	DLS		*Zeta Potential (mV)	pI
		Particle size(nm)	PDI		
Silica-NIPAm/AA	water	340 ± 18	0.659	-20.60± 4	4.05
	Sea water	90 ± 5	0.141		
TiO <sub>2</sub> -NIPAm/AA	water	520± 35	0.373	-27.47± 3	5.1
	Sea water	68± 15	0.171		
Na-MMT-NIPAm/AA	water	700± 25	0.187	-33.13± 7	3.5
	Sea water	80± 15	0.231		

\*The all measurements were carried out in 10<sup>-3</sup> M KCl at pH 7

It was also confirmed that pH 7 is suitable to obtain stable NIPAm/AA nanogel composites which had negative  $\zeta$ -potential values up to -32 mV ( Na-MMT-NIPAm/AA), which stabilized the colloidal particles effectively. The negative  $\zeta$ -potential values of NIPAm/AA nanogel composites are



referred to ionization of carboxylic groups of AA at pH values above 3.3, which resulted in the negative net charge of the nanogel composites. The low negative  $\zeta$ -potential values of silica at pH 4 leads to aggregation of silica nanogel composites particles due to neutral surface charge, caused by the complete masking of the carboxylic groups of AA nanogel composites. These measurements can concluded that the nanomaterials coated with nanogel composites produce stabilized nanomaterials having less polydispersity and smaller size when nanogel composite have both high thickness and high degree of crosslinking density as observed in  $\text{TiO}_2$ -NIPAm/AA and Na-MMT-NIPAm/AA nanogel composites.

### 3.2. Curing of nanogel composites with epoxy matrix

The prepared Na-MMT, silica and titania NIPAm/AA nanogels were dispersed in epoxy resins with different weight percentages ranged from 0.1 to 3.0 Wt % as illustrated in the experimental section. The dispersed Na-MMT silica and titania NIPAm/AA nanogels in epoxy resin were cured with polyamide hardener according to recommended volume ratio. The remained hydroxyl groups of titania and silica on nanoparticles surfaces can interact with amide or epoxy groups of hardener and resin, respectively via hydrogen bonding or polar/polar interactions [48]. The electrostatic interaction between surface charges of MMT silicate layers and amide or epoxy groups will occur during the curing of epoxy and clay galleries [49]. The dispersion of Na-MMT, silica and titania NIPAm/AA nanogels in epoxy matrix can be examined by optical microscope of glass coated with cured epoxy nanogel composites as represented in Figure 4 a-d.

Smooth surface is observed for cured epoxy resins in absence of nanogel composites (Figure 4 a). The Na-MMT, silica and titania NIPAm/AA nanogels showed different dispersion efficiencies depend on the types and contents of nanogel composites. The addition of  $\text{TiO}_2$  -NIPAm/AA (Figure 4 b) shows good dispersion at different weight percentages, although the size of particles increased at 3 Wt %. The formation of agglomerate clusters appears in silica -NIPAm/AA (Figure 4 c) above 0.1 Wt %. The formation of highly dispersed and exfoliated Na-MMT-NIPAm/AA epoxy matrix is observed (Figure 4d). These data can be referred to higher surface charges (Table 2) at the surface of Na-MMT and  $\text{TiO}_2$  NIPAm/AA nanogels which increases the repulsion between the particles and inhibit their agglomerations.

The measuring of cured epoxy coats wettability is very important parameter that determines the diffusion of fluid into the coats that affects anticorrosive performance of coats. In this respect, the contact angles measurements between sea water and epoxy coats were determined and summarized in Table 3 and as selected in Figure 5 a-d. The data confirm that all contact angles between coats and sea water increase with incorporation of nanocomposite more than blank. This means that the Na-MMT, silica and titania NIPAm/AA nanogels form hydrophobic surfaces attributed to outer shell nanogel that contains polymer backbone and isopropyl groups. The hydroxyl groups of both epoxy and nanoparticles interacted with epoxy matrix and directed to interact of the substrate surface [50].

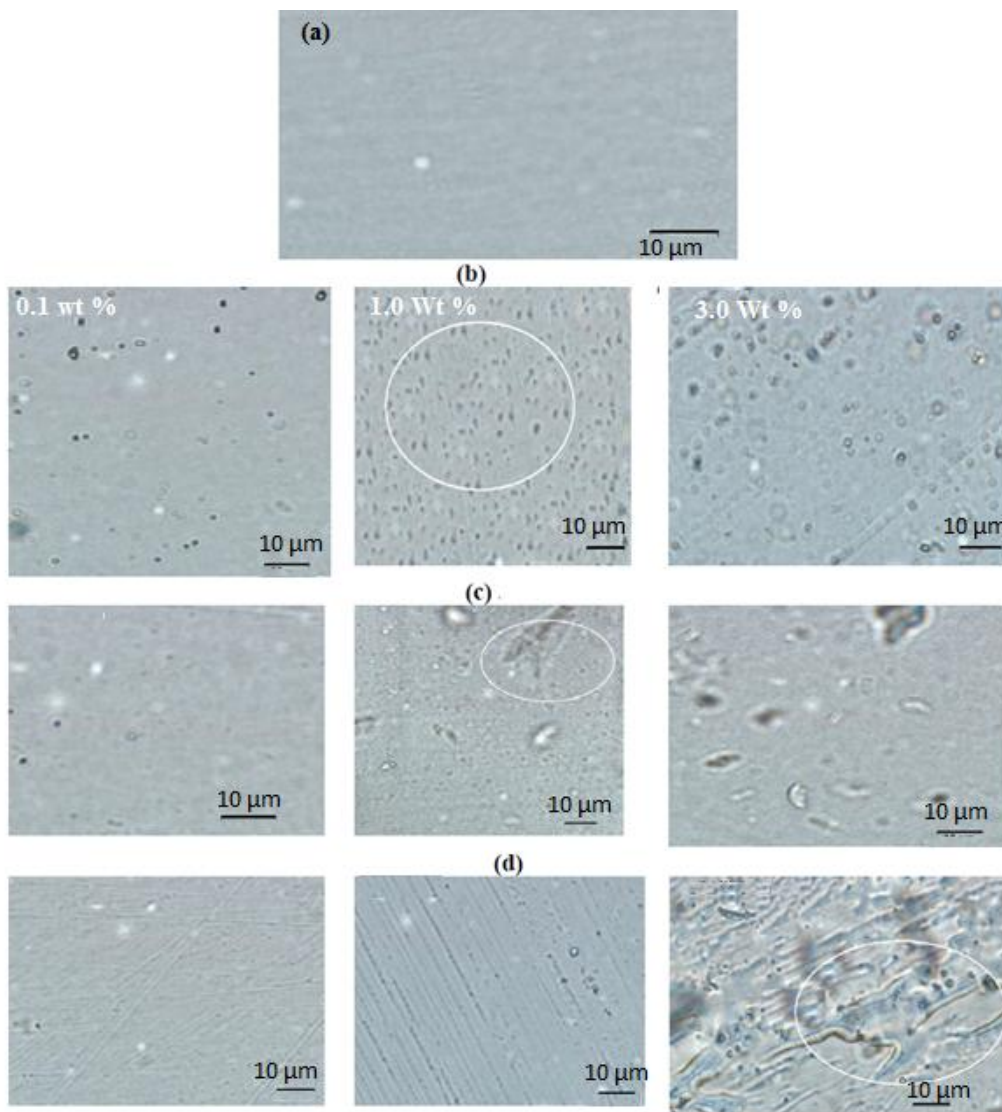


**Figure 4.** Optical microscope micrographs of cured epoxy in the absence and presence of different wt % of a) blank, b) TiO<sub>2</sub>-NIPAm/AA, c) silica-NIPAm/AA, and d) Na-MMT-NIPAm/AA nanogels

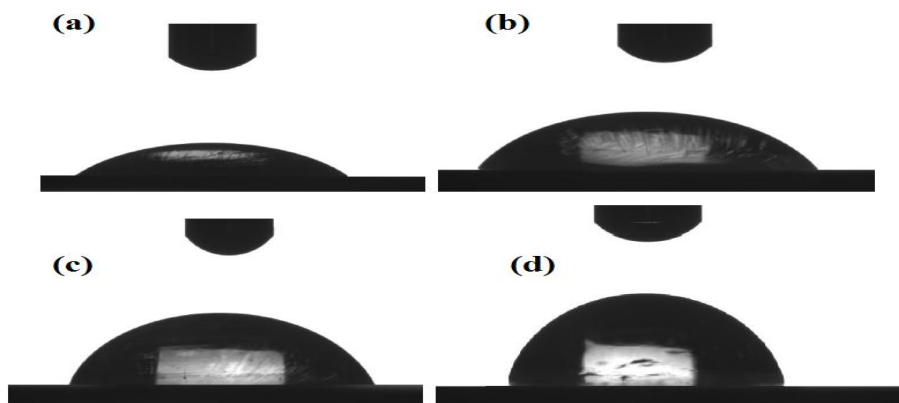


**Figure 5.** Contact angles photos between sea water and cured epoxy surfaces in the presence of a) blank, b) 0.1, c) 1.0 and d) 3.0 Wt % of Na-MMT-NIPAm/AA nanogel composites.

**Table 3.** Contact angle data between sea water and cured epoxy surfaces in the presence of NIPAm/AA nanogel composites.

Cured epoxy	Concentrations of nanocomposites (Wt %)	Contact angles (degree)
blank	0	45
Na-MMT-NIPAm/AA	0.1	78.33
	1.0	79.70
	3.0	95.9
TiO <sub>2</sub> -NIPAm/AA	0.1	61.5
	1.0	70.83
	3.0	88.75
silica-NIPAm/AA	0.1	61.70
	1.0	65.23
	3.0	53.5

The higher dispersion of NIPAm/AA nanogels produces high contact angle values as reported in Table 3. The high dispersion of NIPAm/AA nanoparticles increases the inter-molecular hydrogen bonding between amide groups of NIPAm and COOH of AA to produce more hydrophobic surfaces due to increment of hydrophobic interaction between isopropyl groups.

### 3.3 Mechanical and Anticorrosion performances of cured epoxy matrix with nanogel composites

The strong adhesion between organic coats and steel substrate is very important to improve their coating performance. It is well established that the curing of epoxy resins with polyamide hardeners produces hydroxyl groups that are responsible on the adhesion of epoxy coats with steel substrates as well as amide groups of hardeners [51]. Moreover, the steel surfaces possess positive charges which required coats possess negative surface charges to increase the adhesion of coat with steel substrate. In this respect, the adhesion pull-off tester has been used to evaluate the adhesion of cured epoxy resins with steel substrate and the data were summarized in Table 4. The data confirm that, the epoxy modified with different weight percentages of Na-MMT, silica and titania NIPAm/AA nanogels have good adhesion with steel substrate than unmodified epoxy resins. Moreover, the adhesion of epoxy coats modified with Na-MMT-NIPAm/AA nanogel composites have greater adhesion pull-off resistance forces than that modified with silica and titania NIPAm/AA nanogels. These data can refered to increase electrostatic attraction between epoxy modified coats that possesses more negative surface charges ( Table 2) and positive charges on the steel substrate as well as the exfoliation of Na-MMT nanogel composites increases the negative charges on the exfoliated Na-MMT gallery[52]. The increment of adhesion between steel and epoxy coats contain TiO<sub>2</sub>-NIPAm/AA more than that contain silica- NIPAm/AA nanogels confirms that the high dispersability of nanomaterials in epoxy coats increases the adhesion forces between hydroxyl groups on the titania with steel more than that obtained at silica surfaces.

The mechanical properties of epoxy coats such as impact, abrasion resistances, hardness force and bending tests were determined and listed in Table 4. The data confirm that the mechanical properties of epoxy coats modified with Na-MMT, silica and titania NIPAm/AA nanogels have excellent mechanical properties than that unmodified (blank). These mean that the dispersion of nanomaterials into epoxy matrix improves the mechanical properties of coats. Moreover, the modification of nanomaterials based on Na-MMT, silica and titania as core with flexible nanogel shell based on NIPAm/AA enhances the mechanical properties of epoxy coats to improve their impact and abrasion resistances (Table 4).

**Table 4.** Mechanical properties of cured epoxy with different types of NIPAm-AA nanogel composites.

Sample		Pull-off resistance (MP)	Impact test (Joule)	Hardness (Newton)	Bending	Abrasion resistance mg / 1kg weight for 1000 cycles
Blank		4	5	8	pass	72
TiO <sub>2</sub> -NIPAm/AA	0.1%	12	14	12	pass	15
	1%	14	15	13	pass	18
	3%	16	17	14	pass	20
silica-NIPAm/AA	0.1%	8	11	10	pass	20
	1%	9	14	12	pass	26
	3%	7	13	11	pass	31
Na-MMT-NIPAm/AA	0.1%	14	15	13	pass	13
	1%	17	17	14	pass	15
	3%	19	19	16	pass	19

This can also refer to greater absorption of flexible nanomaterials to impact and abrasion forces improves also the hardness of the modified epoxy coats with Na-MMT, silica and titania NIPAm/AA nanogels.

The anticorrosion characteristics of modified epoxy coats for steel surfaces against salt and water can be examined by salt spray resistance test. The results of salt spray tests of modified epoxy coats at different duration times ranged from 300 to 1000h and their photos were summarized and represented in Table 5 and Figure 6a-d. The data elucidate that, the presence of nanomaterials based on Na-MMT, silica and titania NIPAm/AA nanogels increases the duration exposure times of coats to salt spray more than unmodified epoxy coats. This can be referred to these nanoparticles can fill the cracks, microscopic porosities and free volumes existed in the epoxy coating matrix leading to the increase of electrolyte pathway length due to their smaller particle sizes in sea water ( Figure 3 and Table 2). However, the nanomaterials based on Na-MMT, silica and titania only show barrier role to

protect the epoxy surface and steel from corrosion but they cannot provide protection performance when a mechanical damage like scratch is produced on the coating. Accordingly, the modification of Na-MMT, silica and titania with nanogel aims to overcome this problems.

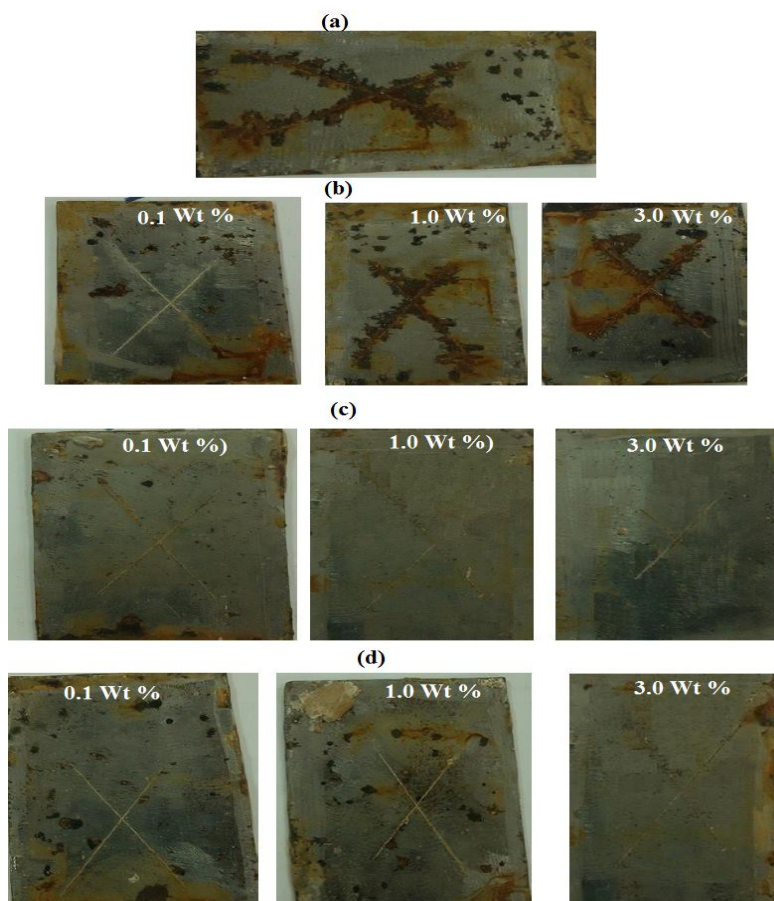


**Figure 6.** Salt spray photos of cured epoxy in the absence and presence of different Wt % of a) blank, b) silica-NIPAm/AA, c) Na-MMT-NIPAm/AA and d) TiO<sub>2</sub>-NIPAm/AA, nanogels having different duration times.

**Table 5.** Salt spray resistance of cured epoxy films.

Paint samples	Sample ratio	Exposure time (hours)	Disbonded area %	Rating Number (ASTM D1654)
Na-MMT-NIPAm/AA	0.1%	1000	3	8
	1%	1000	2	8
	3%	1000	1.5	9
TiO <sub>2</sub> -NIPAm/AA	0.1%	750	5	7
	1 %	750	3	8
	3%	750	1	9
Silica-NIPAm/AA	0.1%	500	20	5
	1%	500	30	4
	3%	500	50	2

The photos ( Figure 6 elucidate that the concentrations and type of nanogel composites affect the anticorrosion performance to act as self-healing for epoxy modified coats. It is found that, the unmodified epoxy coat (Figure 6 a) destroy after duration times 300 h with the formation of rust. While the modification of epoxy with silica-NIPAm/AA (Figure 6b) cannot act as self-healing materials due to formation of rust at damage x cut area although the duration time of coats increased to 500 h. It was also found that both Na-MMT and TiO<sub>2</sub> modified with NIPAm/AA ( Figure 6 c and d) show self-healing characteristics due to no rust formations at x-cut area even at low content ( 0.1 Wt %). In our previous works [53-55], the presence of smart nanogel based on NIPAm surrounded to metal oxide increase their ability to form self-heal layer at damage area due to their sensitivity to surrounded aggressive environments to act as anti-corrosion coats. In the present work, the exfoliation of Na-MMT-NIPAm/AA into epoxy matrix and their excellent adhesion to steel substrate increase their activity to inhibit the diffusion of salts or water into epoxy coat to act as water repealed coats as illustrated from contact angle measurements.

#### 4. CONCLUSIONS

The modification of Na-MMT, silica and TiO<sub>2</sub> nanoparticles by nanogel based on NIPAm/AA produce stabilized nanomaterials having low polydispersity index and smaller size when nanogel composite have both high thickness and high degree of crosslinking density as determined in TiO<sub>2</sub>-NIPAm/AA and Na-MMT-NIPAm/AA nanogel composites. The high dispersion of TiO<sub>2</sub>-NIPAm/AA and Na-MMT-NIPAm/AA nanogel composites in epoxy matrix increases the intera-molecular hydrogen bonding between amide groups of NIPAm and COOH of AA to produce more hydrophobic surfaces due to increment of hydrophobic interaction between isopropyl groups. The TiO<sub>2</sub>-NIPAm/AA and Na-MMT-NIPAm/AA nanogel composites succeeded to improve the mechanical properties of cured epoxy films due to the nanogel shell produced elastic nanomaterials have great efficiency to absorb the impact and abrasion resistance. The good adhesion of modified epoxy films with TiO<sub>2</sub>-NIPAm/AA and Na-MMT-NIPAm/AA nanogel composites produce anticorrosive self-healing nanomaterials for damaged area on the surface of cured epoxy coats in marine environments.

#### ACKNOWLEDGEMENT

The project was financially supported by King Saud University, Vice Deanship of Research Chairs.

#### References

1. S.A. Kapole, B.A. Bhanvase, D.V. Pinjari, R.D. Kulkarni, U.D. Patil, P.R. Gogate, S.H. Sonawane, A.B. Pandit, *Comp.Interf.*, 21 (2014) 469 – 486.
2. M. Tyagi, B.A. Bhanvase, S.L. Pandharipande, *Ind. Eng. Chem. Res.*, 53(2014) 9764 – 9771.
3. R.H. Fernando, ACS Symp. Ser. 1008 (2009) 2–21.
4. B. Ramezanzadeh, E. Ghasemi, M. Mahdavian, E. Changizi, M.H. Moghadam, *Carbon*, 93 (2015) 555–573.
5. L. Xue, L. Xu, Q. Li, *J. Mater. Sci. Technol. (Shenyang, China)*, 23 (2007) 563–567.

6. M. Gharagozloua, B. Ramezanzadehb, Z. Baradarana, *Appl. Surf. Sci.*, 377 (2016) 86–98.
7. D.G. Shchukin, H. Möhwald, *Adv. Funct. Mater.*, 17 (2007) 1451–1458.
8. B.A. Bhanvase, Y. Kutbuddin, R.N. Borse, N.R. Selokar, D.V. Pinjari, P.R. Gogate, S.H. Sonawane, A.B. Pandit, *Chem. Eng. J.*, 231 (2013) 345–354.
9. S.H. Sonawane, B.A. Bhanvase, A.A. Jamali, S.K. Dubey, S.S. Kale, D.V. Pinjari, R.D. Kulkarni, P.R. Gogate, A.B. Pandit, *Chem. Eng. J.*, 189–190 (2012) 464–472.
10. L. Ma, F. Chen, Z. Li, M. Gan, J. Yan, S. Wei, Y. Bai, J. Zeng, *Compos, Part B: Eng.*, 58 (2014) 54–58
11. X. Yuan, Z.F. Yue, X. Chen, S.F. Wen, L. Li, T. Feng, *Corros. Sci.*, 104 (2016) 84–97.
12. S. Sharifi Golru, M. M. Attar, B. Ramezanzadeh, *Prog. Org. Coat.*, 77 (9) (2014) 1391–1399.
13. J. Li, L. Ecco, M. Fedel, V. Ermini, G. Delmas, J. Pan, *Prog. Org. Coat.*, 87 (2015) 179–188.
14. B. Ramezanzadeh, M.M. Attar, *Corrosion*, 69(8) (2013) 793–803.
15. R.R. Moraes, J.W. Garciab, M. D. Barros, S. H. Lewis, C.S. Pfeifer, J. C. Liuc , J. W. Stansbury, *Dental Materials*, 27 (2011) 509–519.
16. N.B. Graham, A. Cameron, *Pure Appl. Chem.*, 70 (1998)1271–1275.
17. M. Ballauff, Y. Lu, *Polymer*, 48(2007)1815–1823.
18. A. Fernandez-Barbero, I. J. Suarez, B. Sierra-Martin, A. Fernandez-Nieves, F. J. de las Nieves, M. Marquez, *Adv. Colloid Interface Sci.*, 147–48 (2009) 88–108.
19. J.E. Wong, A.K. Gaharwar, D. Muller-Schulte, D. Bahadur, W. Richtering, *J. Colloid Interface Sci.*, 324 (2008) 47–54.
20. A.M. Atta, G.A. El-Mahdy, H.A. Al-Lohedan, K.R. Shoueir, *Int. J. Electrochem. Sci.*, 10 (2015) 870–882.
21. M. A. Akl, A. M. Atta, A.M. Yousef and M. I. Alaa, *Polymer International, Polym Int.*, 62(2013)1667–1677.
22. A. M. Atta, R. A. M. El-Ghazawy, R. K. Farag, S. M. Elsaed, *Polym. Advanc. Technol.*, 22 (5) (2011) 732–737.
23. A. M. Atta, G. A. El-Mahdy, H. A. Al-Lohedan, A. O. Ezzat, *Molecules*, 19(2014)10410-10426.
24. M. Motornov, R. Sheparovych, R. Lupitskyy, E. MacWilliams, S. Minko, *J. Colloid Interface Sci.*, 310 (2007) 481–8.
25. M. Motornov, R. Sheparovych, R. Lupitskyy, E. MacWilliams, S. Minko, *Adv. Mater.*, 20 (2008)200–205.
26. M. Motornov, R. Sheparovych, R. Lupitskyy, E. MacWilliams, O. Hoy, I. Luzinov, *Adv. Funct. Mater.*, 17 (2007)2307–2314.
27. G. A. El-Mahdy, A. M. Attaa, H. A. Al-Lohedan, *J. Taiwan Instit. Chem. Eng.*, 45(4) (2014)1947-1953.
28. A.M. Atta, G. A. El-Mahdy, H. A. Al-Lohedan, A. O. Ezzat, *J. Mol. Liq.* 211 (2015) 315–323.
29. A. Atta, H. A. Al-Lohedan, G. El Mahdy, A. O. Ezzat, *Journal of Nanomaterials*, Article ID 580607, 8 pages <http://dx.doi.org/10.1155/2013/580607> (2013).
30. A. M. Atta, O. E. El-Azabawy and H.S. Ismail, *Corros. Sci.*, 53 (2011)1680–1689.
31. A. M. Atta , G. A. El-Mahdy, H. A. Al-Lohedan and S.A. Al-Hussain, *Int. J. Mol. Sci.*, 15 (2014) 6974-6989.
32. D. O. Grigoriev, K. Kohler, E. Skorb, D. G. Shchukin, H. Mohwald, *Soft Matter*, 5 (2009)1426 – 1432.
33. A. M. Atta, A. K. F. Dyab, and H. A. Allohedan, *Polym. Adv. Technol.*, 24 (11)(2013) 986–996.
34. A. M. Atta, H. A. Allohedan, K. Al-Hadad, *RSC Advances*, 6 (2016) 41229 – 41238.
35. A. M. Atta, H. A. Allohedan, *Polym. Sci. series B*, 55 (2013) 233–239.
36. A. M. Atta, *Polym Int* 63 (2014) 607–615.
37. G.A. El-Mahdy, A.M. Atta, H.A. Al-Lohedan, A.M. Tawfeek, A. A. Abdel-Khalek, *Int. J. Electrochem. Sci.*, 10 (7) (2015) 5702-5713.



38. A. M. Atta, H. A. Al-Lohedan, Z. A. AlOthman, A. A. Abdel-Khalek, A. M. Tawfeek, *J. Ind. Eng. Chem.*, 31(2015) 374-384.
39. A. M. Atta, H. A. Al-Lohedan, A. M. Tawfeek, A. A. Abdel-Khalek, *Digest J. Nanomat. Biostructure*, 10 (3) (2014)1087-1102.
40. G.A. El-Mahdy, A.M. Atta, H.A. Al-Lohedan, A.M. Tawfeek, A. A. Abdel-Khalek, *Int. J. Electrochem. Sci.*, 10 (2015)151-161.
41. A. M. Atta, H. A. Al-Lohedan, A. M. Tawfik and A.O. Ezzat, *Molecules* , 21(10) (2016)1392; doi:10.3390/molecules21101392
42. A.V. Delgado, F. Gonzalez-Caballero, R. Hunter, L. Koopal, J. Lyklema, *J. Colloid Interface Sci.* 309 (2007)194-224.
43. G.B. Sukhorukov, E. Donath, S. Davis, H. Lichtenfeld, F. Caruso, V. I. Popov, H. Möhwald, *Polym. Adv. Technol.*, 9 (1998) 759-767.
44. N. T. Qazvini, S. Zinatloo, *J. Mater. Sci. Mater. Med.*, 22(2011) 63-69.
45. M. J. Tiera, G. R. dos Santos, V. A. de Oliveira, N. A. Blaz Vieira, E. Frolini, R. C. da Silva, W. Loh, *Colloid Polym. Sci.*, 283 (2005)662–670 DOI 10.1007/s00396-004-1198-9.
46. F. Danhier, N. Lecouturier, B. Vroman, C. Jérôme, J. Marchand-Brynaert, O. Feron, V.Préat, *J. Controlled Release*, 133(2009)11-17.
47. D.B. Shenoy, M.M. Amiji, *Int. J. Pharm.*, 293 (2005) 261-270.
48. Y. Sun, Z. Zhang and C. P. Wong, *Polymer*, 46 (2005). 2297-2305
49. P.B. Messersmith, E.P. Giannelis, *Chem. Mater.*, 6 (1994) 1719-1725.
50. H. Zou, S. Wu and J. Shen, *Chem. Rev.*, 108 (9) (2008)3893–3957.
51. R.S. Baur, *advances in chemistry*. Washington (DC): American Chemical Society; 1979. p. 144.
52. K. M. Söderholm, *Coatings*, 2 (2012) 138-159.
53. A. M. Atta, H. A. Al-Lohedan, K. Al-Hadad, *RSC Advances*, 6 (2016) 41229 – 41238.
54. A. M. Atta, A. M. El-Saeed, G. M. El-Mahdy, H. A. Al-Lohedan, *RSC Advances*, 5 (123) (2015) 101923-101931.
55. A. M. Atta, A. M. El-Saeed, H. I. Al-Shafey and G. A. El-Mahdy, *Int. J. Electrochem. Sci.*, 11(2016)5735-5752.

© 2017 The Authors. Published by ESG ([www.electrochemsci.org](http://www.electrochemsci.org)). This article is an open access article distributed under the terms and conditions of the Creative Commons Attribution license (<http://creativecommons.org/licenses/by/4.0/>).